Using High Frequency Amateur Radio Transmissions to Detect and Study Travelling Ionospheric Disturbances.

Diego F. Sanchez KD2RLM[1,3], Nathaniel A. Frissell W2NAF[2], Gareth W. Perry KD2SAK[3], William D. Engelke AB4EJ[4], Anthea Coster[5], Philip J. Erickson W1PJE[5], J. Michael Ruohoniemi[6], and Joseph Baker[6], Carl Luetzelschwab K9LA

[1]Essex County College
[2]University of Scranton
[3]New Jersey Institute of Technology
[4]University of Alabama
[5]MIT Haystack Observatory
[6]Virginia Tech

dsanch18@email.essex.edu

Traveling Ionospheric Disturbances

- **TIDs are Quasi-periodic Variations of F Region Electron Density**
- **Medium Scale (MSTID)**
  - $T \approx 15 – 60$ min
  - $v_H \approx 100 – 250$ m/s
  - $\lambda_H \approx$ Several Hundred km (< 1000 km)
  - Often Meteorological Sources
- **Large Scale (LSTID)**
  - $\lambda_h > 1000$ km
  - $30 < T$ [min] < 180
  - Often Auroral Electrojet Enhancement, Particle Precipitation
- **Often associated with Atmospheric Gravity Waves**

[*Francis*, 1975; *Hunsucker* 1982; Ogawa et al., 1967; *Ding* et al., 2012; *Frissell et al.*, 2014; 2016]

dsanch18@email.essex.edu

Data Sources

- **Ham Radio**
  - Reverse Beacon Network
  - Weak Signal Propagation Reporting Network (WSPRNet)
- **SuperDARN**
- **Madrigal GPS Total Electron Content (TEC)**
- **NASA OMNI Data**
- **Ionosonde foF2 Data**

dsanch18@email.essex.edu

Traveling Ionospheric Disturbances

MSTIDs are a type of HF Fading

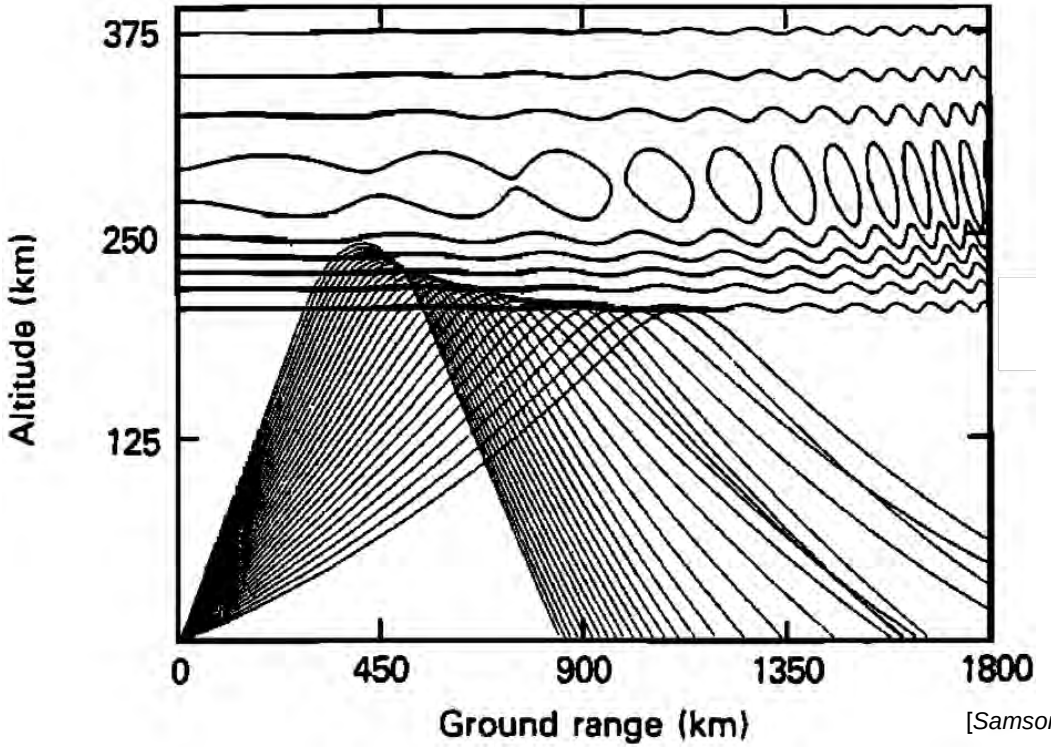

[*Samson et al.*, 1990]

TIDs in Blackstone SuperDARN

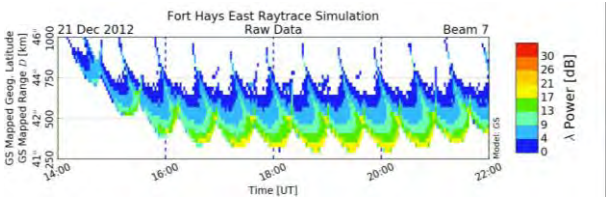

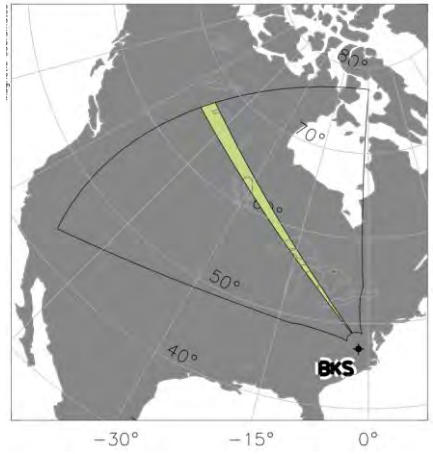

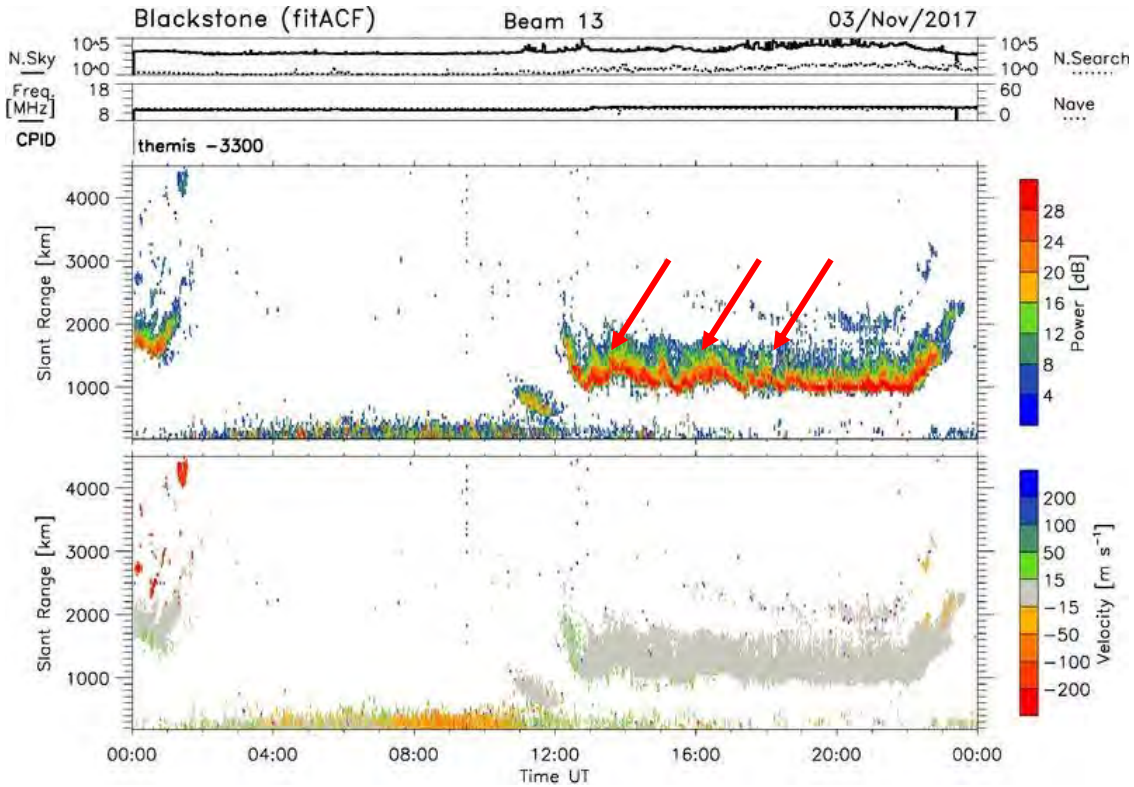

dsanch18@email.essex.edu

Ham Radio TIDs

N Spots = 157559
RBN: 29%
WSPRNet: 71%

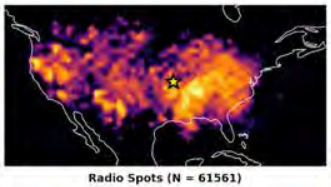

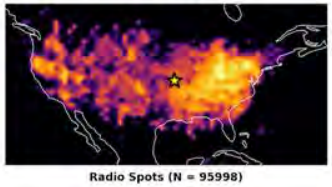

(a) K_p Index

(b) GOES X-Ray

(c) 14 MHz

(d) 7 MHz

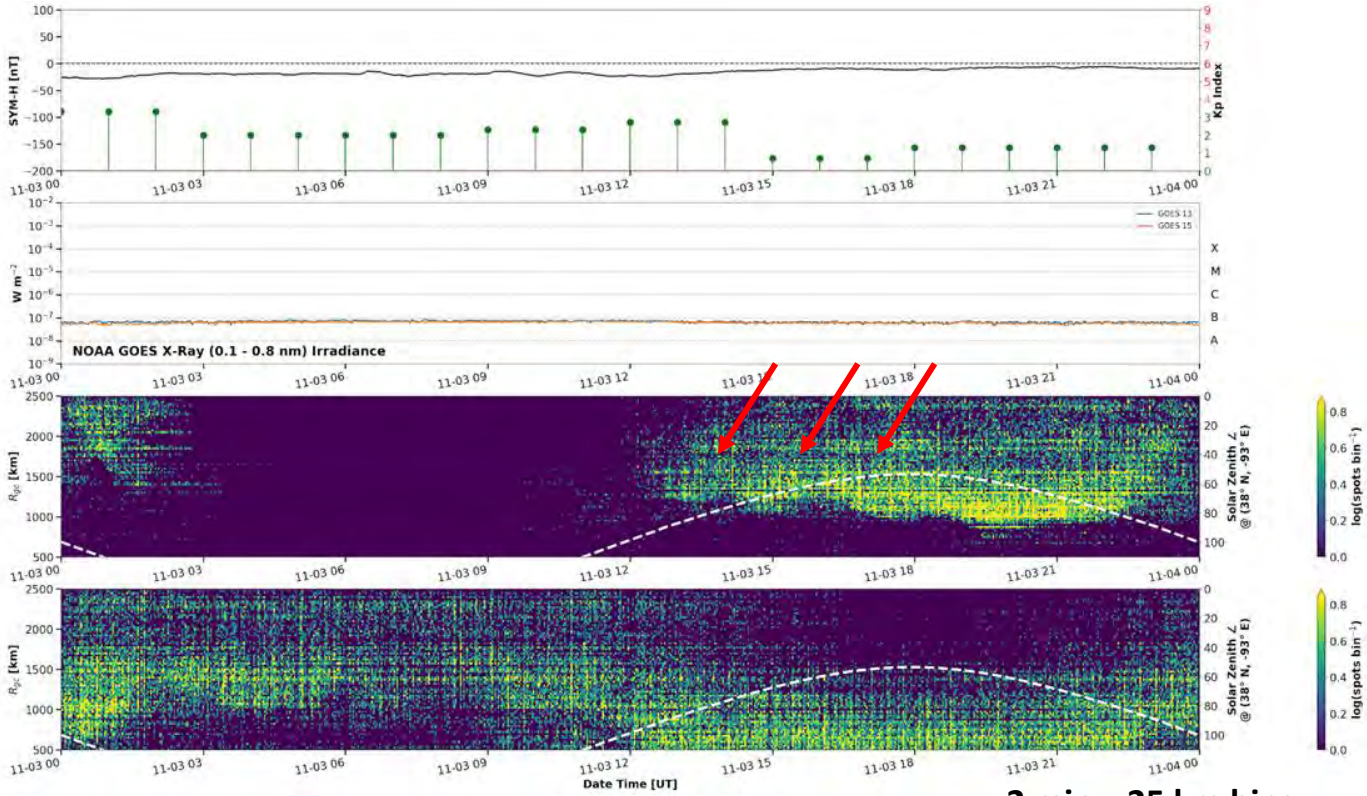

2 min x 25 km bins

dsanch18@email.essex.edu

GNSS TEC Comparison 15:00 - 18:00

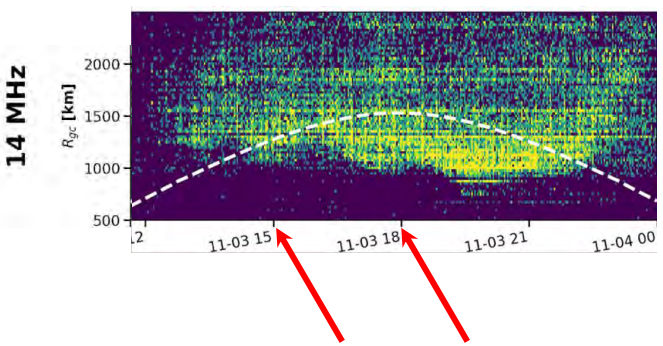

- Radio range is shortest when TEC is red (higher TEC)

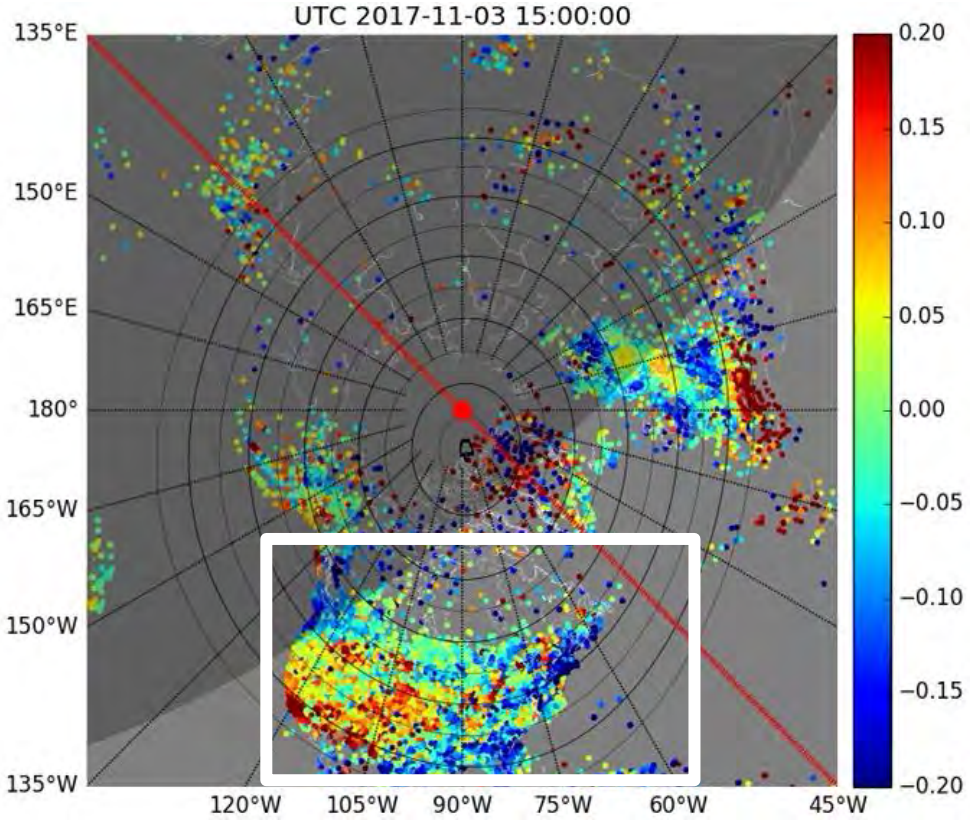

dsanch18@email.essex.edu

GNSS TEC Comparison 18:00 - 21:00

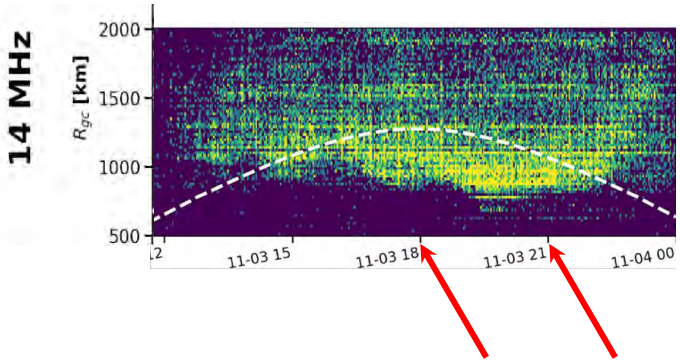

- Radio range is shortest when TEC is red (higher TEC)
- Higher electron densities → More HF refraction, communication range decreases

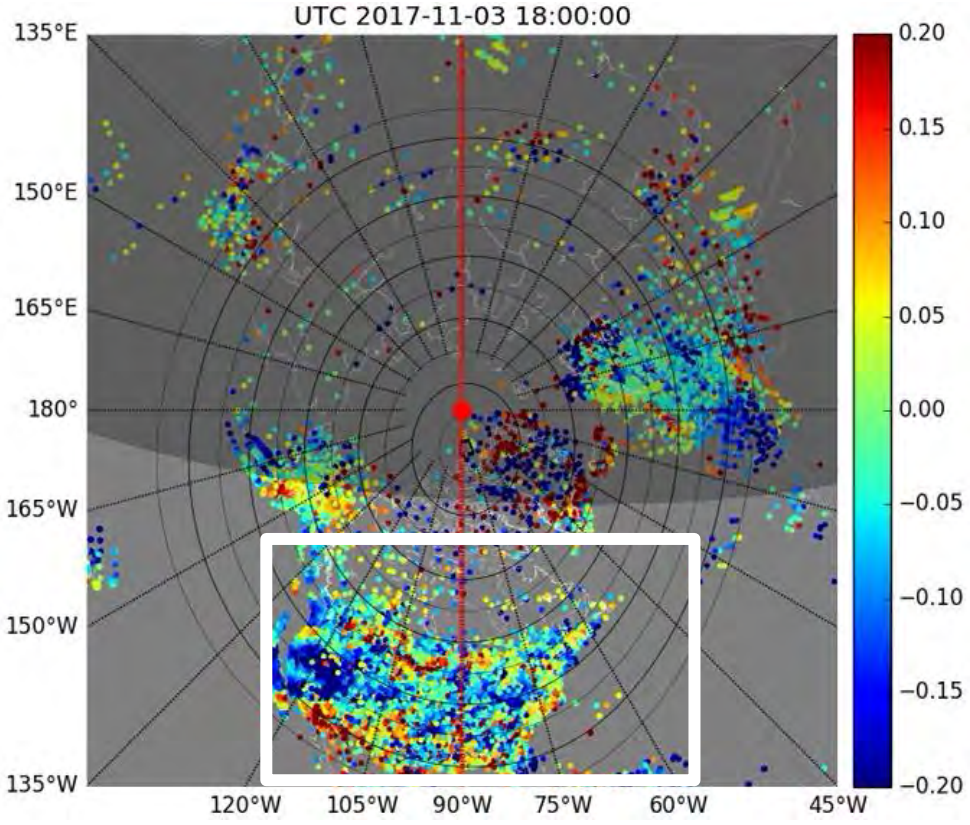

dsanch18@email.essex.edu

Ionosonde Data

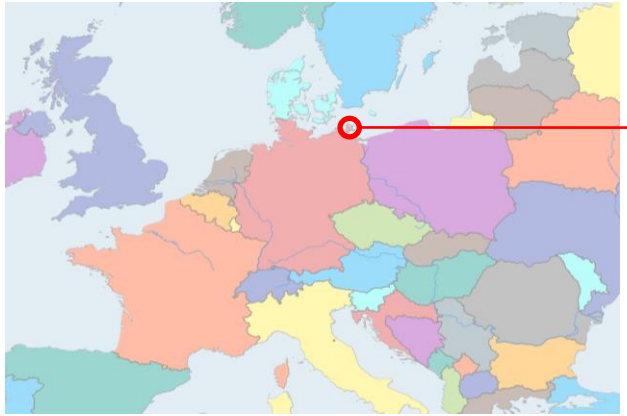

Juliusruh Ionosonde
Rügen, Germany

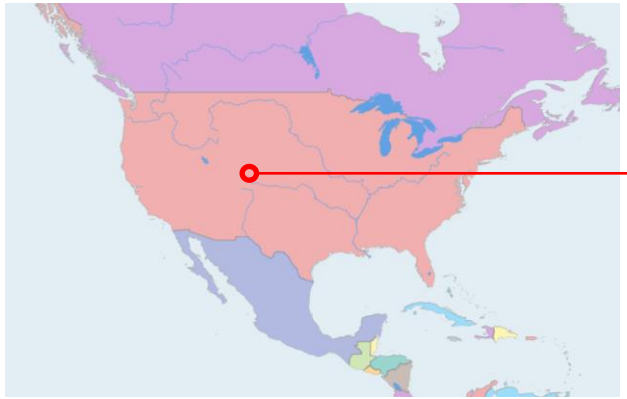

Boulder Ionosonde
Colorado, USA

- Chose ionosondes relatively close to the largest concentration of radio spots.

Jan 26, 2017 14 MHz

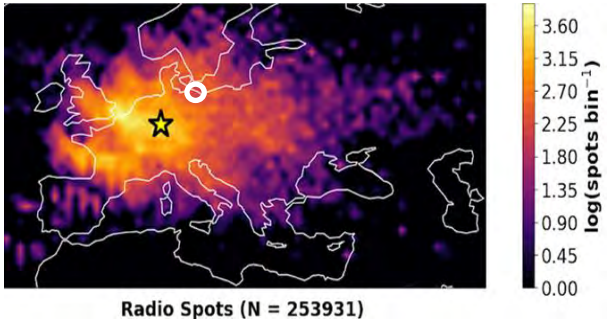

Sep 27, 2017 14 MHz

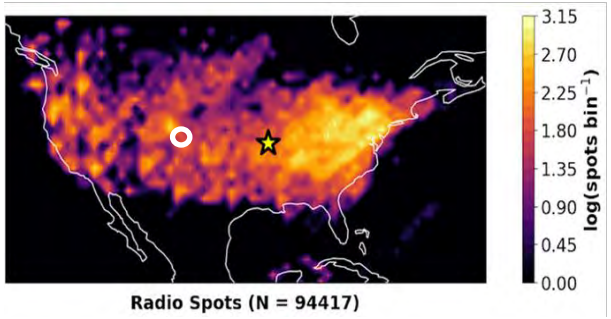

dsanch18@email.essex.edu

January 26, 2017 foF2 Comparison US

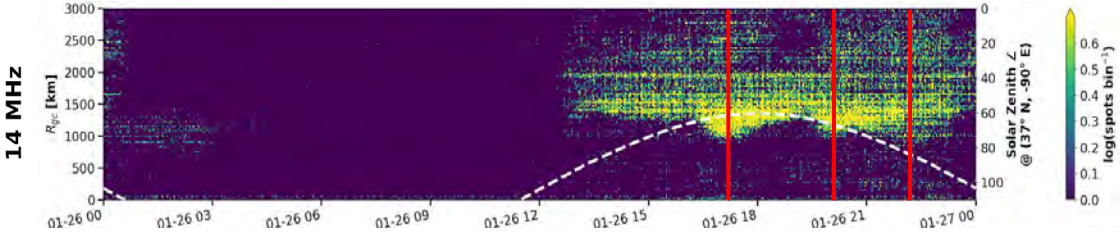

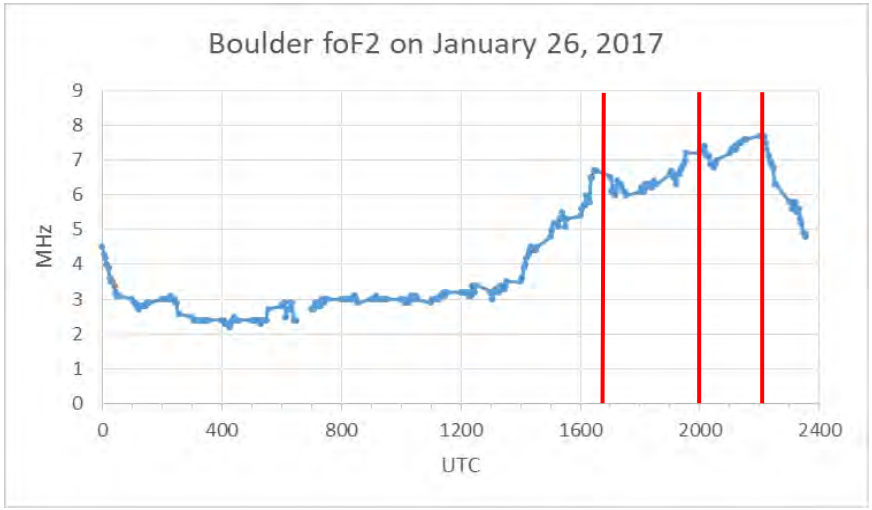

- The highest frequency that the ionosonde reflects is called foF2.
- The higher the frequency that is bounced back from the ionosphere, the higher the electron densities will be.
- More refraction at higher electron densities.
- Radio range is shortest at higher foF2 values.

dsanch18@email.essex.edu

September 27, 2017 foF2 Comparison Europe

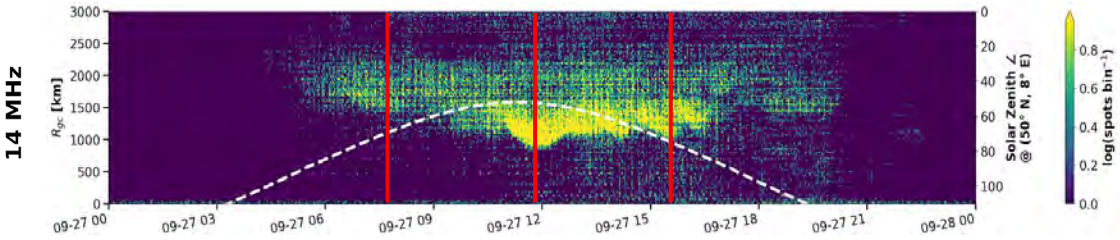

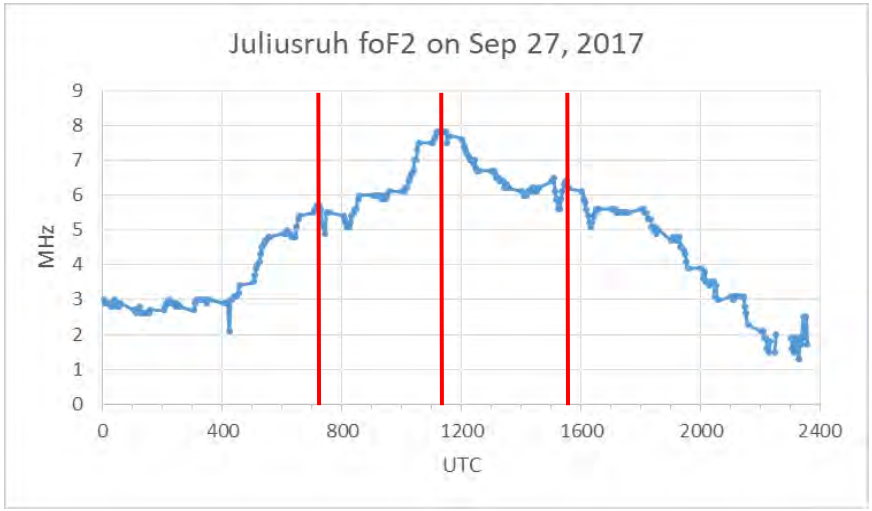

- The highest frequency that the ionosonde reflects is called foF2.
- The higher the frequency that is bounced back from the ionosphere, the higher the electron densities will be.
- More refraction at higher electron densities.
- Radio range is shortest at higher foF2 values.

dsanch18@email.essex.edu

Europe TID Activity

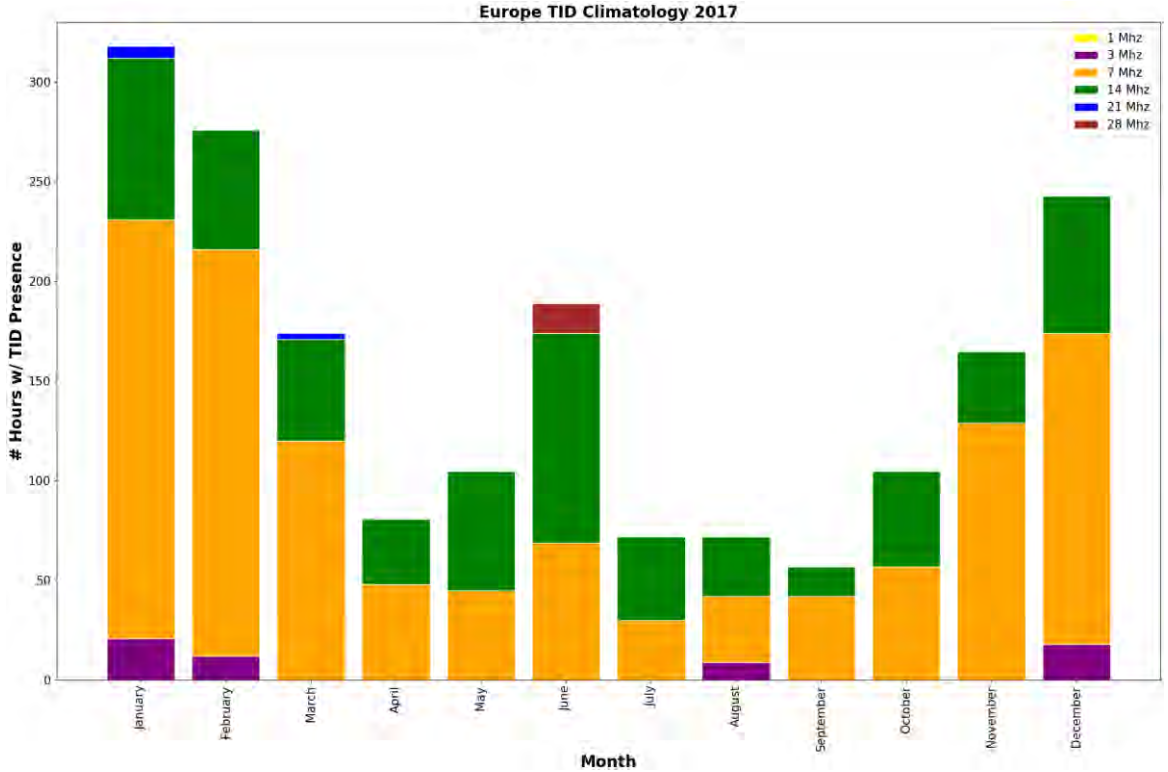

Figures showing the total number of hours with TID activity by month observed within daily ham radio observation plots.

•Data Sources:
- RBN
- WSPRNet

•Date Range:
- 2017

•Geographic Locations:
- Europe

•Bands:
- 1.8 MHz
- 3.5 MHz
- 7 MHz
- 14 Mhz
- 21 MHz
- 28 MHz

•Window Length:
- 1 Hour

dsanch18@email.essex.edu

US TID Activity

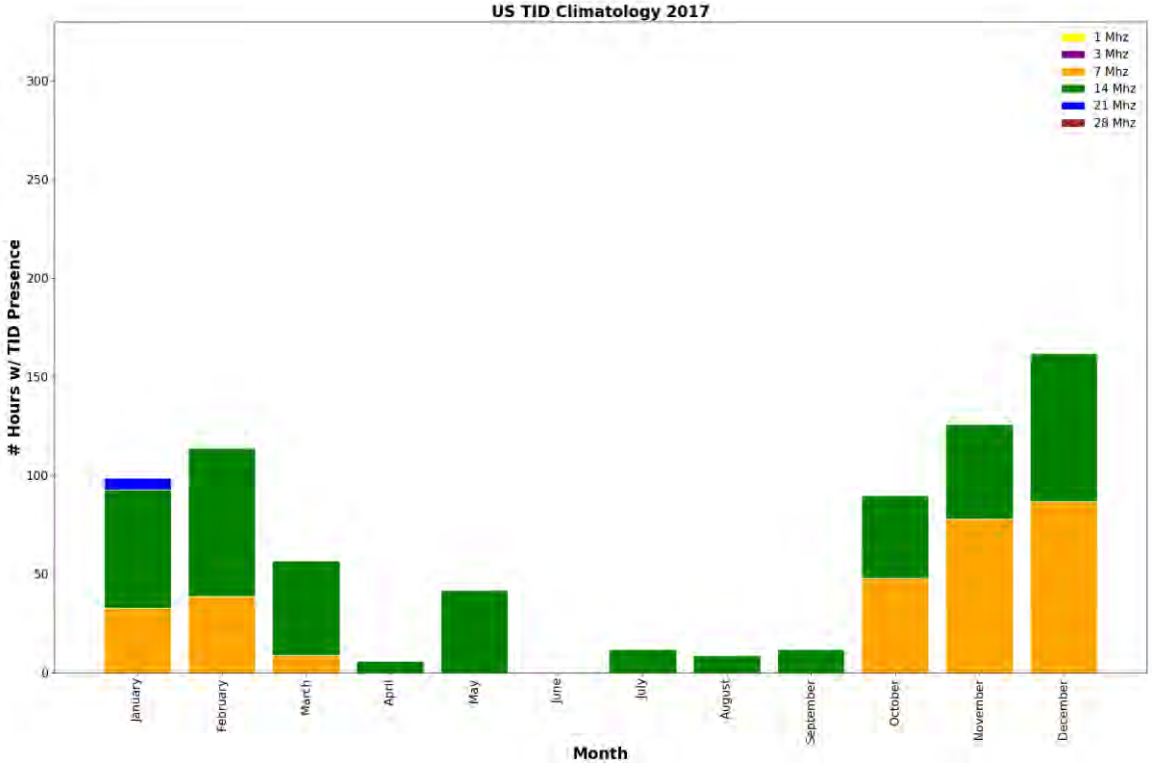

Figures showing the total number of hours with TID activity by month observed within daily ham radio observation plots.

•Data Sources:
- RBN
- WSPRNet

•Date Range:
- 2017

•Geographic Locations:
- Europe

•Bands:
- 1.8 MHz
- 3.5 MHz
- 7 MHz
- 14 Mhz
- 21 MHz
- 28 MHz

•Window Length:
- 1 Hour

dsanch18@email.essex.edu

Europe Total Spot Activity

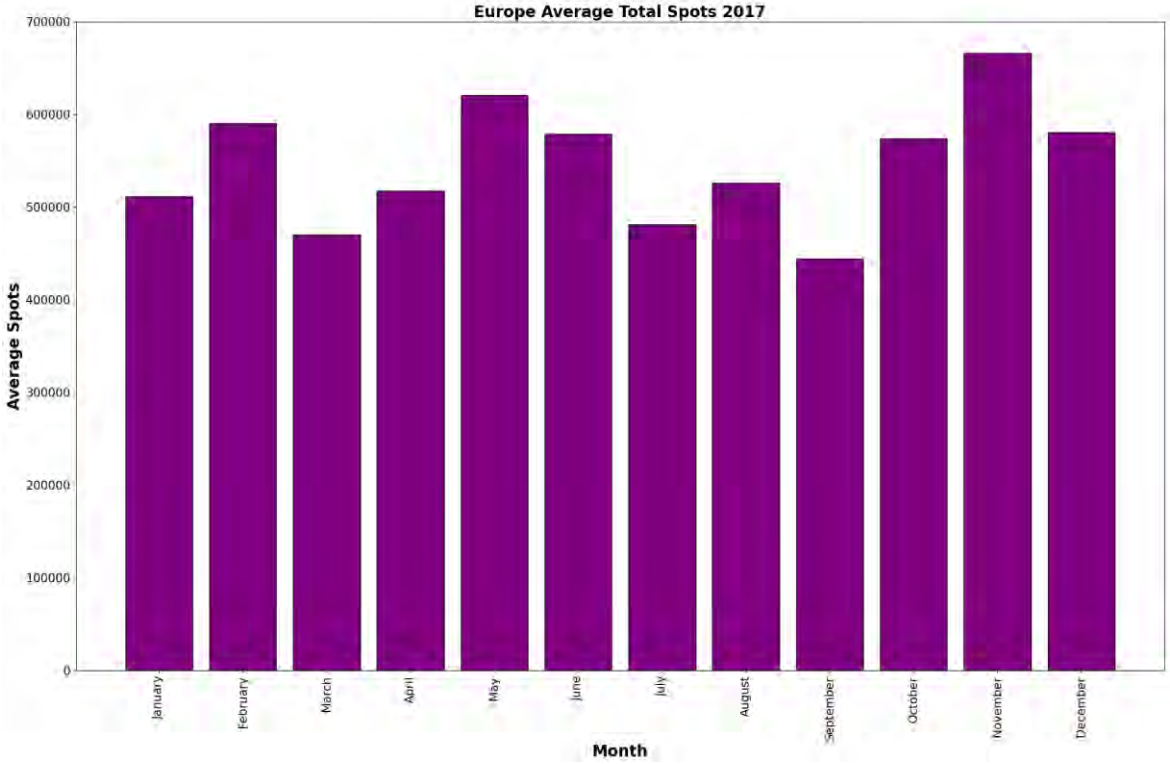

Daily average number of total spots in Europe for the year 2017.

- Relative consistency in the number of spots.
- No noticeable decrease in ham radio activity in the summer months.

dsanch18@email.essex.edu

US Total Spot Activity

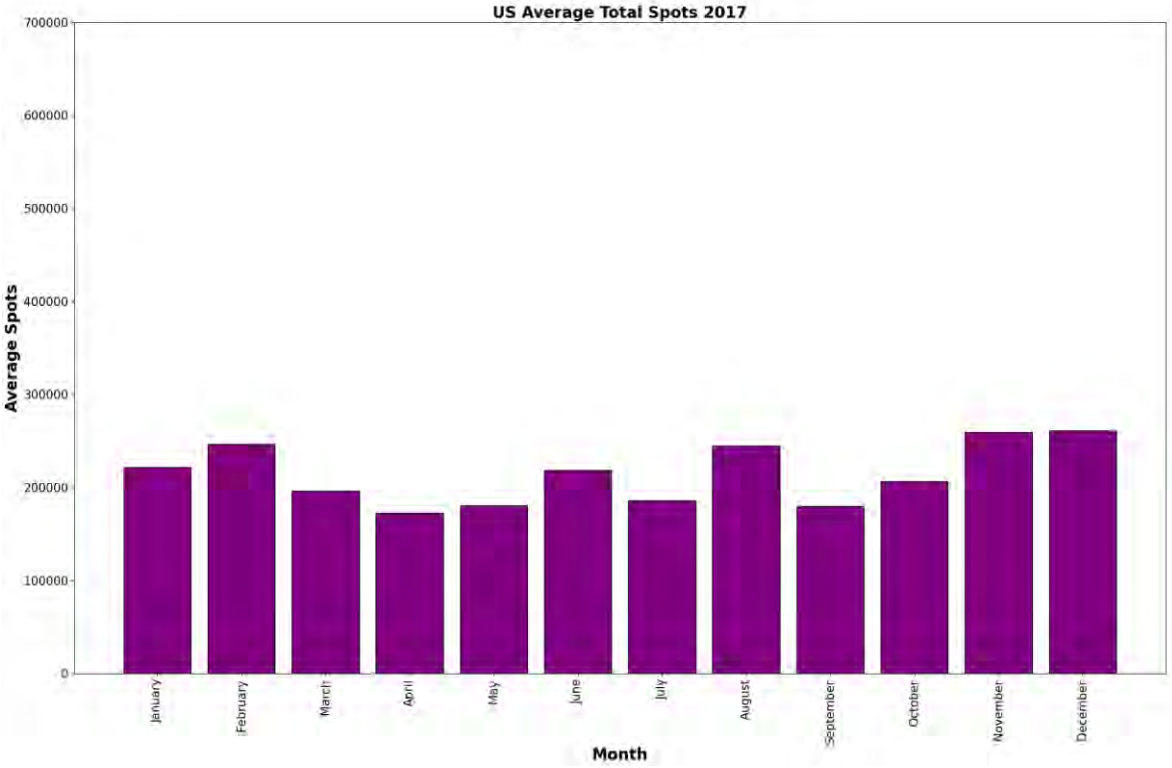

Daily average number of total spots in Europe for the year 2017.

- Relative consistency in the number of spots.
- No noticeable decrease in ham radio activity in the summer months.

dsanch18@email.essex.edu

US Auroral Electrojet Activity

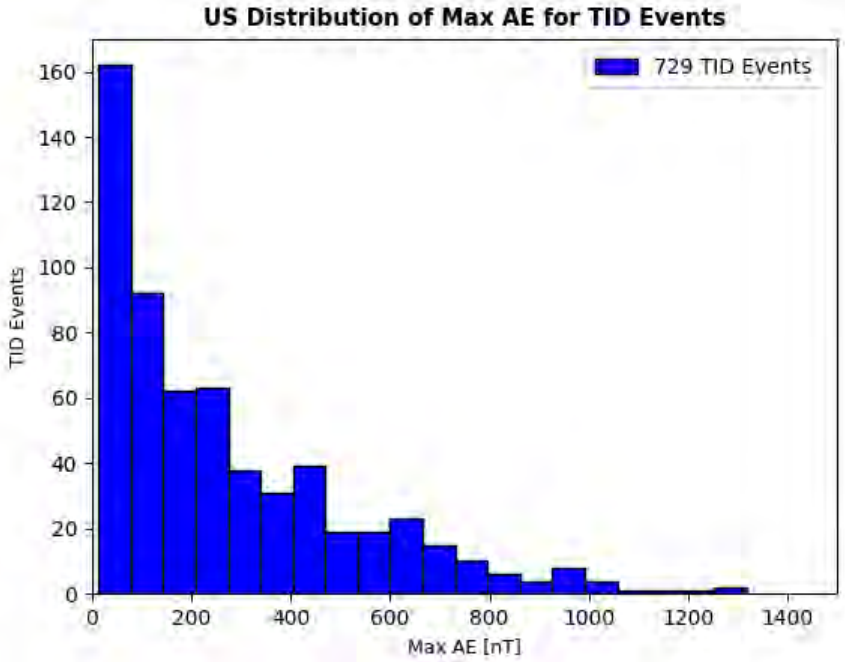

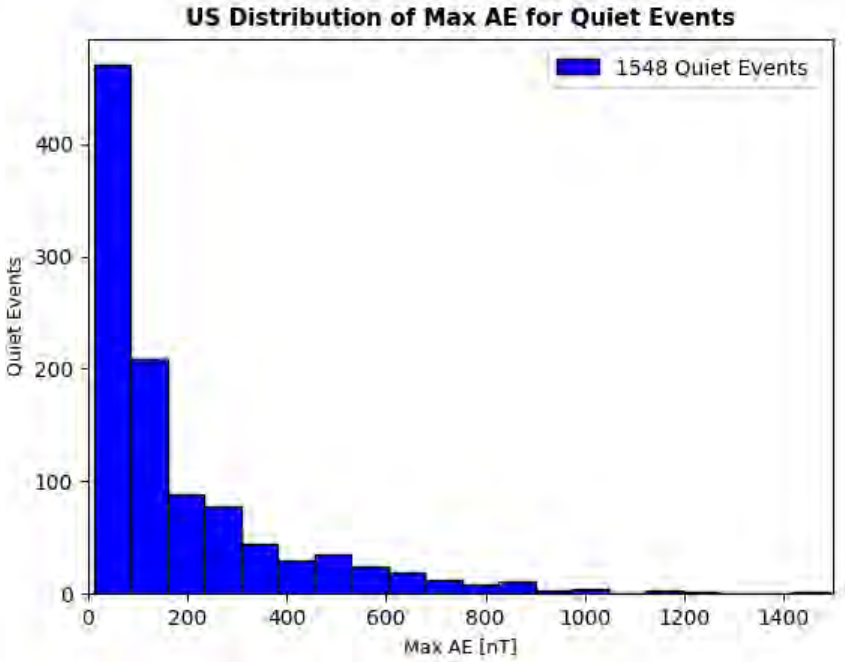

dsanch18@email.essex.edu

European Auroral Electrojet Activity

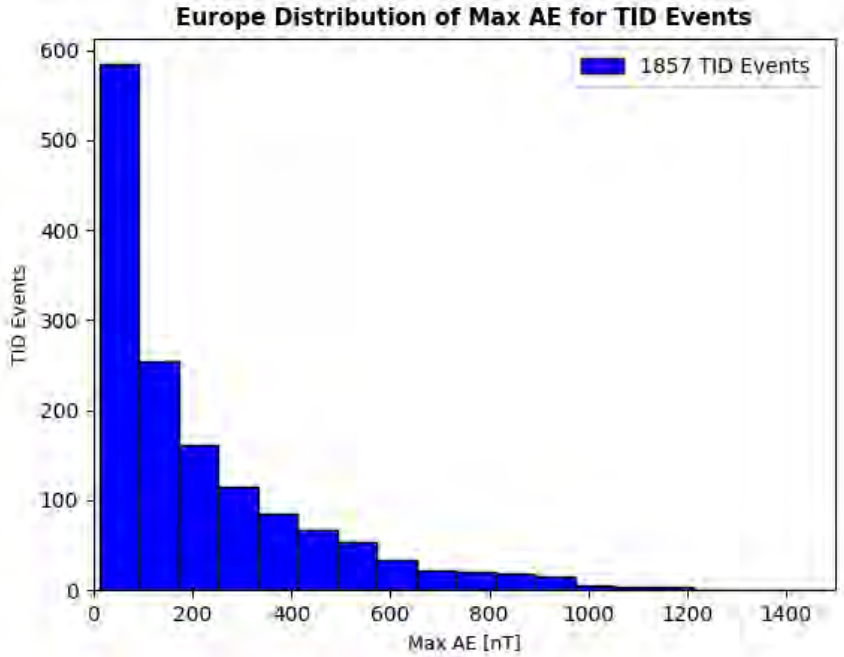

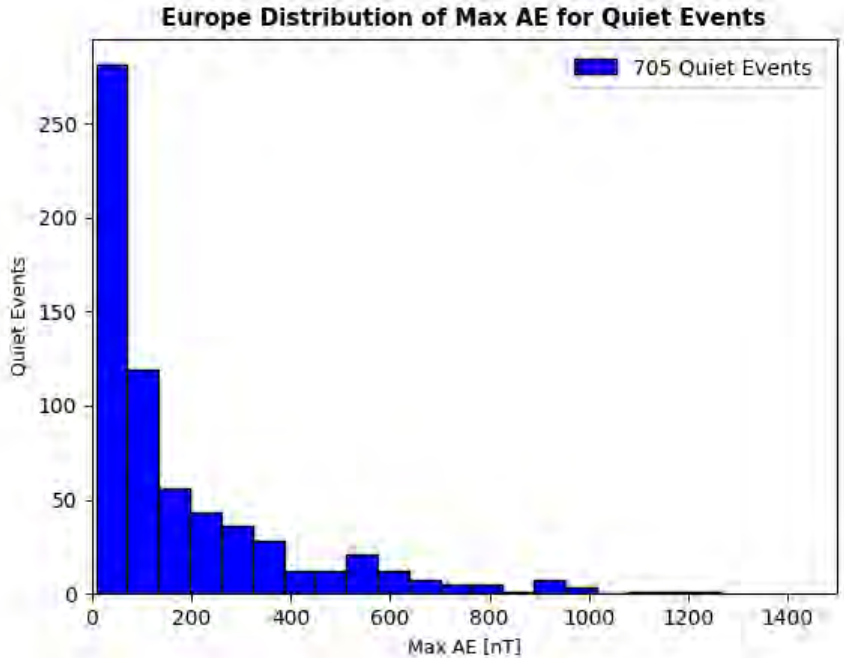

dsanch18@email.essex.edu

US Sym-H Activity

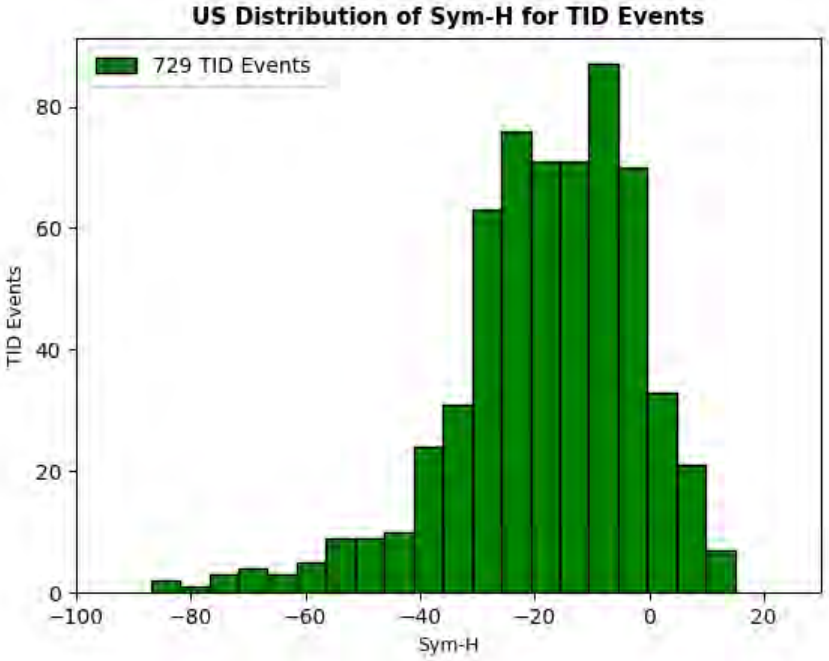

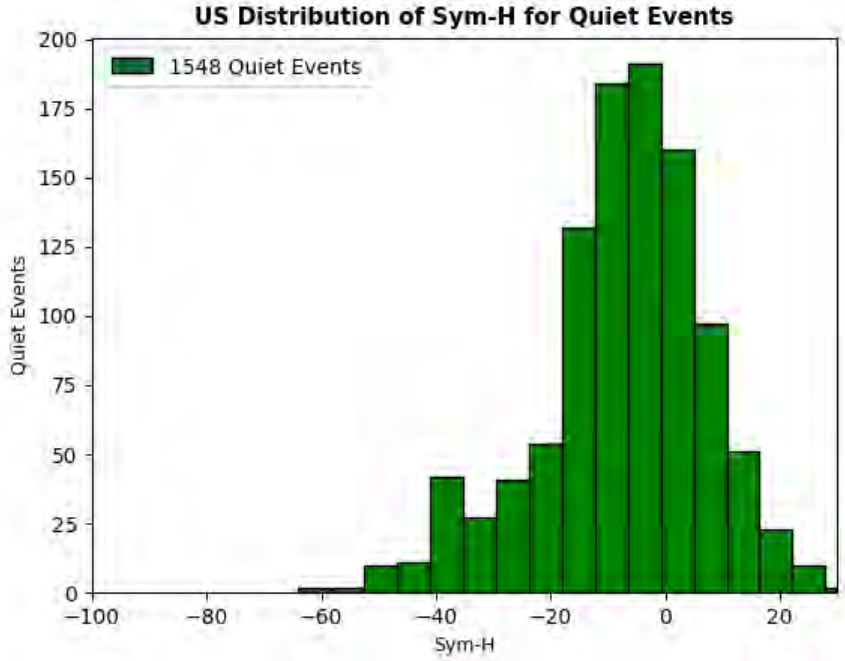

dsanch18@email.essex.edu

European Sym-H Activity

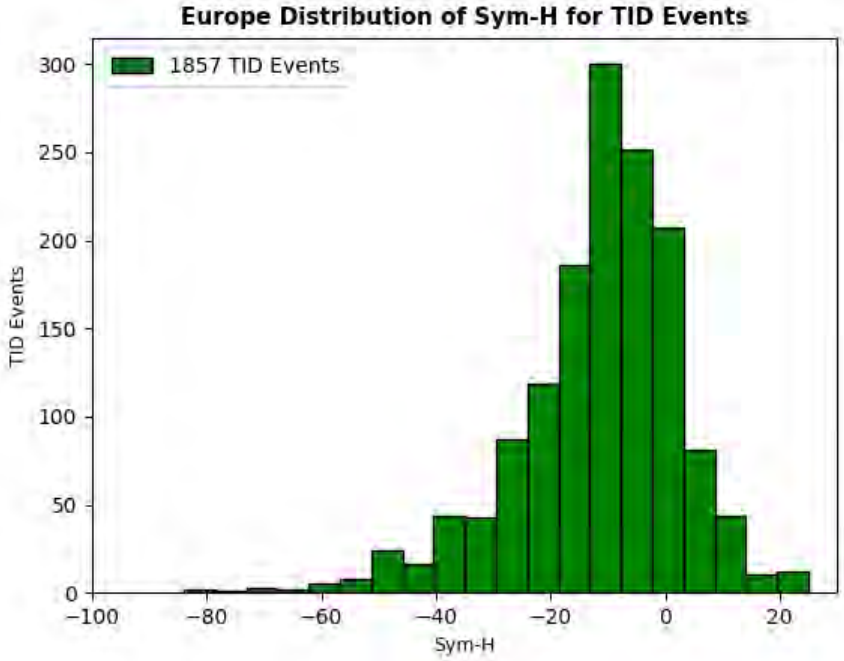

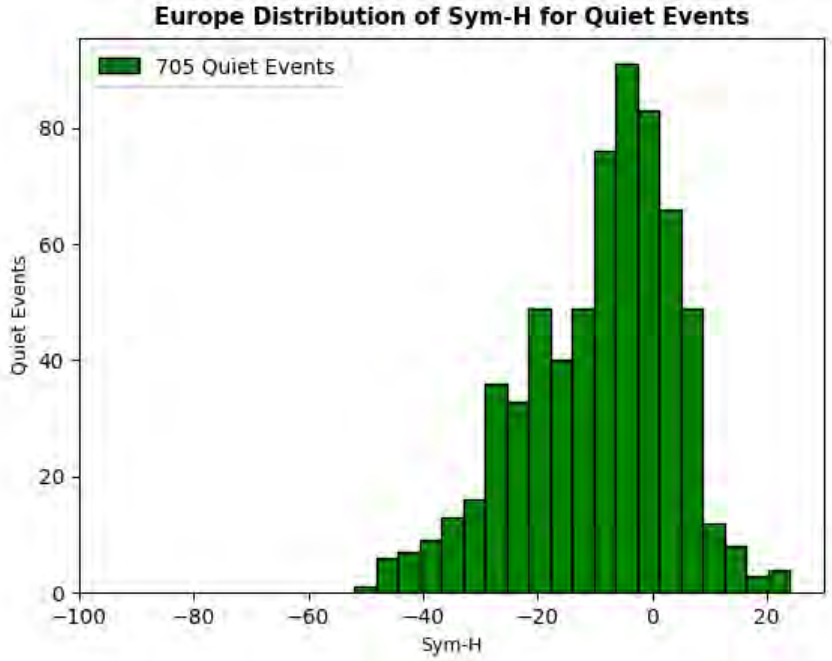

dsanch18@email.essex.edu

Conclusions and Future Work

- Ham Radio Disturbances seem likely to be LSTIDs.
  - Appear coherent across Continental US and Europe.
  - Consistent with BKS SuperDARN Beam 13.
  - Consistent with GNSS TEC.
  - GNSS dTEC Wave Parameter Estimate for 3 November 2017:
    - λ ≈ 1100 km, vp≈950 km/hr, T≈70 min, Azm≈135°
  - Consistent with Boulder (US) and Juliusruh (Europe) Ionosondes.
- RBN and WSPRNet can serve as a tool for monitoring LSTIDs day and night.
  - LSTIDs are detectable in RBN and WSPRNet observations when data is binned into 2D histograms with 2 min x 25 km bins over the United States and Europe.
  - LSTIDs affect available ham radio communication path lengths.
- Fewer night observation capabilities using 14 MHz.
- TID activity more prominent starting in late fall and ending in early spring.
- Ham radio traffic not noticeably influenced by season.
- Exact mechanism is uncertain, currently looking at auroral and geomagnetic sources. Initial observations show:
  - Slightly enhanced max AE [nT] for times with TID events.
  - Higher number of TID events falling around a Sym-H value of -20.
- Develop Automated detection system for TID signatures within Ham radio data.

dsanch18@email.essex.edu

References

Ding, F., Wan, W., Ning, B., Zhao, B., Li, Q., Zhang, R., Xiong, B., and Song, Q. (2012), Two-dimensional imaging of large-scale traveling ionospheric disturbances over China based on GPS data, J. Geophys. Res., 117, A08318, doi:10.1029/2012JA017546.

Francis, S. H. (1975), Global propagation of atmospheric gravity waves: A review, J. Atmos. Terr. Phys., 37, 1011–1054, doi:10.1016/0021-9169(75)90012-4.

Frissell, N. A., Baker, J. B. H., Ruohoniemi, J. M., Gerrard, A. J., Miller, E. S., Marini, J. P., West, M. L., and Bristow, W. A. (2014), Climatology of medium-scale traveling ionospheric disturbances observed by the midlatitude Blackstone SuperDARN radar, J. Geophys. Res. Space Physics, 119, 7679– 7697, doi:10.1002/2014JA019870.

Frissell, N. A., Baker, J. B. H., Ruohoniemi, J. M., Greenwald, R. A., Gerrard, A. J., Miller, E. S., and West, M. L. (2016), Sources and characteristics of medium-scale traveling ionospheric disturbances observed by high-frequency radars in the North American sector, J. Geophys. Res. Space Physics, 121, 3722– 3739, doi:10.1002/2015JA022168.

Chimonas, G. (1970), The equatorial electrojet as a source of long period traveling ionospheric disturbances, Planet. Space Sci., 18(4), 583–589, doi:10.1016/0032-0633(70)90133-9.

Vadas, S. L., and H. Liu (2009), Generation of large-scale gravity waves and neutral winds in the thermosphere from the dissipation of convectively generated gravity waves, J. Geophys. Res., 114, A10310, doi:10.1029/2009JA014108.

dsanch18@email.essex.edu

Acknowledgments

We are especially grateful to the amateur radio community who voluntarily produced and provided the HF radio observations used in this presentation, especially the operators of the Reverse Beacon Network (RBN, reversebeacon.net), the Weak Signal Propagation Reporting Network (WSPRNet, wsprnet.org), qrz.com, and hamcall.net. NAF gratefully acknowledges the support of NSF Grant AGS-2002278. We acknowledge the use of the Free Open-Source Software projects used in this analysis: Ubuntu Linux, python, matplotlib, NumPy, SciPy, pandas, xarray, iPython, and others.

GPS TEC data products and access through the Madrigal distributed data system are provided to the community by the Massachusetts Institute of Technology under support from US National Science Foundation grant AGS-1952737. Data for the TEC processing is provided from the following organizations: UNAVCO, Scripps Orbit and Permanent Array Center, Institut Geographique National, France, International GNSS Service, The Crustal Dynamics Data Information System (CDDIS), National Geodetic Survey, Instituto Brasileiro de Geografia e Estatística, RAMSAC CORS of Instituto Geográfico Nacional de la República Argentina, Arecibo Observatory, Low-Latitude Ionospheric Sensor Network (LISN), Topcon Positioning Systems, Inc., Canadian High Arctic Ionospheric Network, Institute of Geology and Geophysics, Chinese Academy of Sciences, China Meteorology Administration, Centro di Ricerche Sismologiche, Système d'Observation du Niveau des Eaux Littorales (SONEL), RENAG : REseau NAtional GPS permanent, GeoNet - the official source of geological hazard information for New Zealand, GNSS Reference Networks, Finnish Meteorological Institute, SWEPOS - Sweden, Hartebeesthoek Radio Astronomy Observatory, TrigNet Web Application, South Africa, Australian Space Weather Services, RETE INTEGRATA NAZIONALE GPS, Estonian Land Board, and Virginia Tech Center for Space Science and Engineering Research.

The authors acknowledge the use of SuperDARN data. SuperDARN is a collection of radars funded by national scientific funding agencies of Australia, Canada, China, France, Italy, Japan, Norway, South Africa, United Kingdom and the United States of America.

dsanch18@email.essex.edu